# Transport properties of polycrystalline type-I Sn clathrates

G. S. Nolas
*Department of Physics, University of South Florida, Tampa, Florida 33620*

J. L. Cohn
*Department of Physics, University of Miami, Coral Gables, Florida 33124*

J. S. Dyck and C. Uher
*Department of Physics, University of Michigan, Ann Arbor, Michigan 48109*

J. Yang
*Materials and Processes Laboratory, General Motors R&D and Planning, Warren, Michigan 48090*
(Received 6 February 2001; revised manuscript received 18 May 2001; published 4 April 2002)

Thermal conductivity, resistivity, Seebeck coefficient, and Hall measurements on polycrystalline Sn-clathrate compounds with the type-I hydrate crystal structure are reported. Interstitial alkali-metal atoms in these compounds reside inside polyhedral cavities formed by the tetrahedrally bonded Sn network atoms. Localized disorder associated with ''rattling'' motion of these interstitial atoms contributes to the low thermal conductivity of these semiconducting compounds. The Hall coefficient and resistivity for some compounds exhibit nonmonotonic temperature dependences consistent with a crossover with decreasing temperature from conduction-band to impurity-band conduction. The carrier mobility is found to be low even in the absence of interstitial atoms within the Sn framework, suggesting a large effective mass and/or scattering rate. We discuss the properties in the context of potential thermoelectric applications.

DOI: 10.1103/PhysRevB.65.165201 PACS number(s): 72.20.Pa, 66.70.+f

## INTRODUCTION

Semiconducting compounds with a clathrate hydrate-type crystal structure are of growing interest as potential thermoelectric materials. Transport properties of semiconductor type-I Si and Ge clathrates reveal low thermal conductivity values along with relatively high Seebeck coefficients and electronic conductivity.[1–3] The crystal structure of these clathrate compounds consists of a framework of group-IV atoms having several polyhedral ''cages,'' each of which can incorporate relatively large ''guest'' atoms. The thermal conductivities for some of these crystalline compounds have temperature dependences and magnitudes similar to that of amorphous materials.[1–5] This unusual behavior of the thermal transport for the group-IV clathrates (as well as for clathrate hydrates[6]) is attributed to guest-host interactions, whereby the localized guest vibrations interact strongly with the host acoustic modes.[4,5,7,8] The guest translational vibration (or ''rattling'') frequencies increase as the size difference between guest atom and host polyhedra decreases, reflecting the stronger restoring forces acting on guest atoms. The experimental trends in thermal conductivity are similar to those found in the skutterudite material system[9] and are most interesting in terms of thermoelectric applications. They indicate that semiconductors with good electronic properties can be synthesized with ''glasslike'' thermal conductivity.

Sn-clathrates may be of particular interest for thermoelectric cooling applications. Theoretical calculations on ''empty'' type-I and type-II Si-clathrates ($Si_{46}$ and $Si_{136}$, respectively) indicate a band gap of almost 2 eV, substantially larger than that of diamond-structured Si (1.1 eV) and a consequence of the open clathrate structure.[10] Recent band structure calculations suggest this band gap opening also occurs in the case of Sn-clathrates, with type-I alkali-metal compounds being semiconductors.[11] Sn-clathrates may therefore be synthesized to possess narrow band gaps, a prerequisite for thermoelectric cooling materials.[12] The transport properties reported here indicate that the Sn compounds are conventional semiconductors, with guest atoms contributing to an impurity band.

With very few exceptions[2,3,13–15] most of the work thus far on the transport properties of these types of compounds has focused on Si or Ge as the framework atoms. In this work we investigate the transport properties of several Sn-clathrates with the type-I hydrate crystal structure with the aim of investigating their potential for thermoelectric applications.

## SAMPLE PREPARATION AND EXPERIMENTAL PROCEDURE

The basic structural and chemical properties of the Sn-clathrates synthesized for this report are shown in Table I. The cubic unit cell of the type-I Sn-clathrates ($Pm\bar{3}n$) are made up of two different types of polyhedra, two $Sn_{20}$ dodecahedra, and six $Sn_{24}$ tetrakaidecahedra. The Sn framework atoms form bonds in a tetrahedral arrangement; the polyhedra are covalently bonded to each other by shared faces. The alkali-metal atoms are entrapped inside these polyhedra. This interesting structural arrangement is central to the interesting transport properties observed for these compounds.

Sample preparation varies from quite simple—one need

 ©2002 The American Physical Society

TABLE I. Sn-clathrates prepared for this report indicating the atomic percentages from electron-beam microprobe analysis, the lattice parameter $a_0$, in Å, the grain size $d$ of densified polycrystalline samples in microns, measured density $D_{meas}$ in g/cm$^3$, theoretical x-ray density $D_{theory}$, in g/cm$^3$, and the Hall number at room temperature, $n_H$, in units of $10^{19}$/cm$^3$.

| Compound | Elemental at. % | $a_0$ | $d$ | $D_{meas}$ | $D_{theory}$ | $n_H$ |
|---|---|---|---|---|---|---|
| $Cs_8Sn_{44}$ | 15.6Cs/84.4Sn | 12.105 | 13 | 5.38 | 5.89 | 4.6 |
| $Rb_8Ga_8Sn_{38}$ | 14.9Rb/14.9Ga/70.2Sn | 11.947 | 21 | 4.62 | 5.60 | 1.7 |
| $Cs_8Zn_4Sn_{42}$ | 14.6Cs/7.5Zn/77.8Sn | 12.125 | 11 | 5.56 | 5.88 | 4.1 |
| $Rb_8Zn_4Sn_{42}$ | 14.3Rb/7.2Zn/78.5Sn | 12.112 | 7.0 | 4.55 | 5.55 | 4.8 |
| $Cs_8Zn_4Sn_{37}Ge_5$ | 14.7Cs/7.5Zn/8.4Ge/69.4Sn | 12.068 | 7.7 | 4.85 | 5.75 | |

only look at the Cs-Sn phase diagram to prepare $Cs_8Sn_{44}$ (Ref. 16)—to more involved. A general approach that has resulted in phase-pure specimens consists of mixing high-purity elements in an argon-atmosphere glovebox and then reacting the products for 4 weeks at 550 °C inside a tungsten crucible sealed inside a stainless steel canister. The canister was evacuated and backfilled with high-purity argon before sealing. The resulting compound consisted of small octahedral crystals with a shiny, black metallic luster. The structural and chemical properties of these phase-pure specimens were analyzed by powder x-ray diffraction (XRD) and Rietveld refinement, single-crystal XRD on small single crystals, and optical metallographic and electron-beam microprobe analyses. A detailed description of the synthesis approach and structural analyses have been reported elsewhere.[14,15] For transport measurements these compounds were ground to fine powders and hot pressed inside a graphite die at 380 °C and $2.1\times10^4$ psi for 2.5 h in an argon atmosphere. The hot-pressed pellets were cut with a wire saw in the shape of a parallelopiped $2\times2\times5$ mm$^3$ in size.

Four-probe electrical resistivity ($\rho$), steady-state Seebeck coefficient ($S$), and steady-state thermal conductivity ($\kappa$) measurements were performed in a radiation-shielded vacuum probe ''dipper'' or inside a closed-cycle refrigerator. Heat losses via conduction through lead wires and radiation were determined in separate experiments and the data corrected accordingly. These corrections were 15%–20% near room temperature and $<5\%$ at $T<120$ K. The Hall coefficient ($R_H$) was measured using a 16-Hz Linear Research bridge in conjunction with a cryostat equipped with a 5-T superconducting magnet. Hall resistance was taken in both positive and negative magnetic fields to correct for any misalignment of the Hall probes. The advantage of the ac technique is that it compensates the thermal emf generated within the specimen. Care was taken to polish the specimen surface well before making electrical contact to prevent unwanted conduction from surface defect states.

## RESULTS AND DISCUSSION

Figure 1 shows the lattice thermal conductivity $\kappa_g$ as a function of temperature of five polycrystalline compounds with type-I crystal structure along with data on $n$-type InSb.[17] Thermal conductivity for some of these compounds has been reported previously.[2,13–15] From the measured values of $\kappa$ and $\rho$ we employ the Wiedemann-Franz relation to estimate and subtract the electronic component $\kappa_e$, thus computing the lattice contribution $\kappa_g=\kappa-\kappa_e$ ($\kappa_e=L_0T/\rho$ with $L_0=2.44\times10^{-8}$ V$^2$/K$^2$). The data are also corrected for porosity for the relatively porous polycrystalline specimens (see Table I). The $\kappa_g$ of the $Cs_8Sn_{44}$ specimen exhibits a sharp maximum at $T_{max}\sim10$ K and an approximately $1/T$ dependence for $T>T_{max}$, both typical of crystalline insulators; the high-$T$ behavior is characteristic of phonon-phonon scattering. $\kappa_g$ for both $Cs_8Zn_4Sn_{42}$ and $Rb_8Zn_4Sn_{42}$ also decreases with increasing temperature for $T>T_{max}$, however, not as strongly as for $Cs_8Sn_{44}$, and $T_{max}$ is shifted to higher $T$, presumably due, in part, to mass-fluctuation disorder scattering of the phonons.

Theoretical,[8] structural information,[14,15] and optical measurements[18] corroborate the hypothesis that resonant interaction of guest-host atom vibrations is a mechanism for $\kappa_g$ suppression, suggesting a simple interpretation of the differences in $\kappa_g$ for these compounds. First, consider $Cs_8Sn_{44}$ and $Cs_8Zn_4Sn_{42}$. Both have Cs atoms in cages: however, the former compound has two Sn vacancies per formula unit. The additional bonding between the Cs and Sn atoms neighboring the vacancies in $Cs_8Sn_{44}$ constrains the displacement of Cs atoms in the tetrakaidecahedra, as revealed by recent temperature-dependent neutron scattering data.[15] These data indicate a large thermal motion for Cs in the tetrakaidecahedra of the $Cs_8Zn_4Sn_{42}$ compound, but a thermal motion for

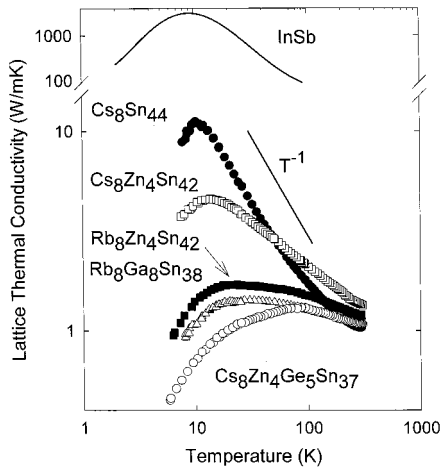


FIG. 1. Lattice thermal conductivity for type-I Sn-clathrates from 5 to 300 K. Data for InSb are plotted for comparison.

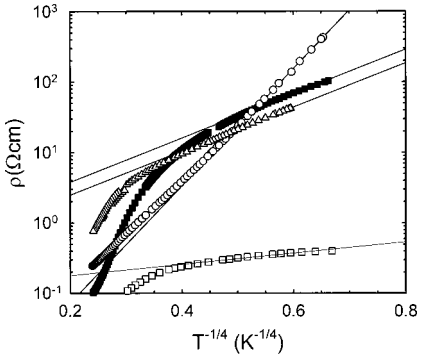


FIG. 2. Resistivity vs $1/T^{1/4}$ for $Rb_8Ga_8Sn_{38}$ (open triangles), $Rb_8Zn_4Sn_{42}$ (solid squares), and $Cs_8Zn_4Sn_{37}Ge_5$ (open circles). Solid lines are linear-least-squares fits of the data for $T<25$ K, with parameters described in the text.

Cs that is similar to that of Sn in the $Cs_8Sn_{44}$ compound. We therefore conclude that the additional atomic displacements are the source of $\kappa_g$ suppression in $Cs_8Zn_4Sn_{42}$ relative to $Cs_8Sn_{44}$. Rb atoms are smaller than Cs atoms, and thus it is expected that Rb will ''rattle'' more freely inside the polyhedra formed by the (Zn,Sn) atoms. These localized vibrations may provide more prominent phonon scattering that is reflected in the still lower $\kappa_g$ of $Rb_8Zn_4Sn_{42}$. While the enhanced thermal motion of the Cs and Rb atoms in these Sn-clathrates appear to diminish $\kappa_g$, the effect is not as great as that caused by the Sr motion in $Sr_8Ga_{16}Ge_{30}$ where the Sr vibration frequencies lie in the range of the acoustic phonons and result in a ''glasslike'' temperature dependence of $\kappa_g$.[1–5,7,8,13,18,19]

Figures 2–4 show $\rho(T)$, $R_H(T)$, and $S(T)$ for several of the samples. All of the Sn-clathrate specimens examined had *n*-type Hall coefficients that were independent of applied magnetic field in the range 0.5–5 T within the error of the measurements. Given these observations, a single-band picture appears applicable to the *n*-type compounds. The $Cs_8Zn_4Sn_{37}Ge_5$ compound had a positive Hall coefficient that was strongly field dependent, suggesting contributions to $R_H$ from more than one band.

Evidence for impurity-band conduction at low $T$ is provided by the observation of variable-range-hopping behavior,[20] $\rho(T)=\rho_0\exp[(T_0/T)^{1/4}]$ below $T=25$ K for $Rb_8Ga_8Sn_{38}$, $Rb_8Zn_4Sn_{42}$, and $Cs_8Zn_4Sn_{37}Ge_5$ (Fig. 2), with $T_0=2.66\times10^3$, $2.74\times10^3$, and $1.34\times10^5$ K and $\rho_0=5.92\times10^{-1}$, $8.88\times10^{-1}$, and $1.58\times10^{-3}$ Ω cm, respectively. The considerably larger $T_0$ and smaller $\rho_0$ for *p*-type $Cs_8Zn_4Sn_{37}Ge_5$ in comparison to values for the *n*-type compounds reflects the different properties of acceptor and donor impurity bands.

The nonmonotonic temperature variation of $R_H$ observed for three of the specimens is characteristic of a transition from the band conduction at high $T$ to impurity-band conduction at low $T$.[21] A maximum in $R_H$ occurs when the impurity-band and conduction-band conductivities become equal. We find that the simplest model capable of reproducing the features of all the transport data self-consistently consists of a parabolic conduction band and a lower-mobility impurity ''band'' (approximated as a discrete level) with donor density $N_d$ at energy $\varepsilon_d$ below the conduction-band edge (inset, Fig. 3). In the limit $\Delta\gg k_BT$ (Δ being the gap energy) hole conduction can be ignored and the equation of charge neutrality describing this situation can be written as[22]

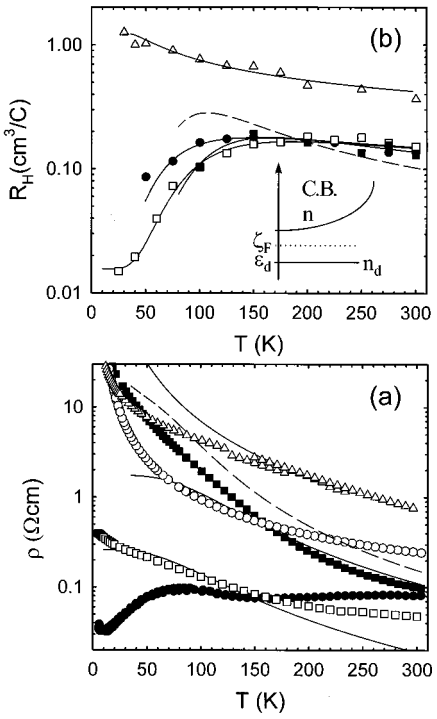


FIG. 3. Resistivity (a) and Hall coefficient (b) vs temperature for $Rb_8Ga_8Sn_{38}$ (open triangles), $Cs_8Sn_{44}$ (solid circles), $Cs_8Zn_4Sn_{42}$ (open squares), $Rb_8Zn_4Sn_{42}$ (solid squares), and $Cs_8Zn_4Sn_{37}Ge_5$ (open circles). The solid curves are fits to the model described in the text, and the dashed curve is for $Rb_8Zn_4Sn_{42}$ with a VRH form for $\mu_d$, with parameters from Table II. The inset depicts the band scheme employed in the model.

$$N_d-n_d=n,$$

$$n_d=\left[1+\frac{1}{2}\exp\left(\eta-\frac{\varepsilon_d}{k_BT}\right)\right]^{-1},$$

$$n=\frac{(2mk_BT)^{3/2}}{2\pi^2\hbar^3}F_{1/2}(\eta),$$

$$F_r=\int_0^\infty\frac{x^r dx}{1+e^{x-\eta}}, \tag{1}$$

where $n_d$ is the electron density in donor states, $n$ is the conduction-band electron density, $\eta=\xi_F/k_BT$, $\xi_F$ is the chemical potential measured with respect to the band edge, and $m$ is the band effective mass. With $N_d$, $\varepsilon_d$, and $m$ employed as adjustable parameters, these equations were solved numerically for $\eta$ with the Hall coefficient and resistivity computed from

$$R_H=\frac{1}{e}\frac{n\mu^2+n_d\mu_d^2}{(n\mu+n_d\mu_d)^2},$$

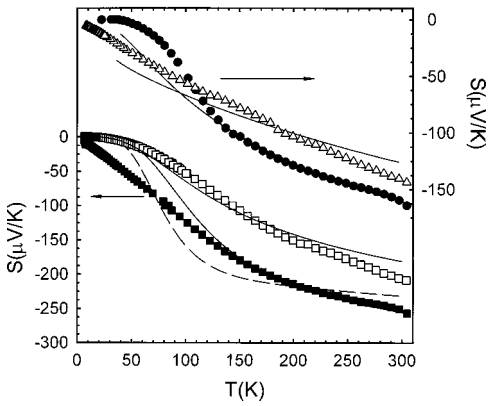


FIG. 4. Thermopower vs temperature for $Rb_8Ga_8Sn_{38}$ (open triangles), $Cs_8Sn_{44}$ (solid circles), $Cs_8Zn_4Sn_{42}$ (open squares), and $Rb_8Zn_4Sn_{42}$ (solid squares). Solid curves are fits to the model described in the text with parameters from Table II. The dashed curve is for $Rb_8Zn_4Sn_{42}$ with a VRH form for $\mu_d$ (also see Table II).

$$\rho = \frac{1}{e(n\mu + n_d\mu_d)}. \tag{2}$$

where $\mu$ and $\mu_d$ are the conduction-band and impurity-band mobilities, respectively. It was assumed that the Hall contribution from the impurity band is *n* type. The total thermopower in this model is given by a weighted sum of the conduction-band ($S$) and impurity-band ($S_d$) contributions,[23]

$$S_{\rm tot} = \frac{Sn\mu + S_d n_d \mu_d}{n\mu + n_d\mu_d},$$

$$S = \frac{k_B}{e}\left(\frac{2+\nu}{1+\nu}\frac{F_{1+\nu}(\eta)}{F_\nu(\eta)} - \eta\right), \tag{3}$$

where $\nu$ is a constant determined by the dominant scattering mechanism ($\nu = 2$, $\frac{1}{2}$, and 0 for ionized impurity, neutral, impurity, and acoustic phonon scattering, respectively).

The scattering mechanism is often determined from the temperature dependence of the Hall mobility, $\mu_H \equiv R_H/\rho$. In the present case, however, we expect the temperature dependence of $\mu_H$ to depend more strongly on the difference in the magnitudes of $\mu$ and $\mu_d$ rather than on their respective temperature dependences. Therefore, to simplify the simultaneous analysis of all three transport coefficients we took $\mu_d$ to be temperature independent and considered temperature-dependent forms for $\mu$ corresponding to ionized impurity ($\propto T^{3/2}$), neutral impurity ($\propto$const), and acoustic phonon scattering ($\propto T^{3/2}$). We also assumed $S_d \ll S$ (a good approximation for $T > 25$ K) such that $S_{\rm tot} \approx S(1 + n_d\mu_d/n\mu)^{-1}$. These simplifications provide for semiquantitative agreement between calculated and measured coefficients; results for ionized impurity scattering are shown as solid curves in Figs. 3 and 4 and fitting parameters presented in Table II.

There is some disagreement between calculated and measured coefficients. The assumption of a constant impurity-band mobility leads to a saturation of the computed resistivity at low $T$ and an underestimate of the measured $\rho$ for $Cs_8Zn_4Sn_{42}$ and particularly for $Rb_8Zn_4Sn_{42}$. Better agreement with the temperature dependence of $\rho$ for $Rb_8Zn_4Sn_{42}$ is achieved in the calculations when a variable-range-hopping (VRH) form (using the same parameters inferred from Fig. 2) for $\mu_d$ is employed (dashed curves in Figs. 3 and 4). Allowing different power-law behaviors for $\mu(T)$ at high and low $T$ allows for excellent fits to both $\rho$ and $R_H$ throughout the temperature range for all specimens, but complicates the analysis of the thermoelectric properties (TEP's) and adds little to the physical picture with the expense of additional parameters. The calculated and measured TEP's are in excellent agreement for $Cs_8Zn_4Sn_{42}$ and less so for the other compounds. We view this as satisfactory given that possible phonon-drag contributions to the TEP have been neglected and $\mu(T)$ has been restricted to a particular power law for all $T$.

For $\nu = 2$ (dominant ionized impurity scattering) the analysis yields $m/m_0 = 0.14$, 0.38, 0.45, and 0.85 for $Rb_8Ga_8Sn_{38}$, $Cs_8Sn_{44}$, $Cs_8Zn_4Sn_{42}$, and $Rb_8Zn_4Sn_{42}$, respectively. Using $\nu = 1/2$ or 0 yielded larger masses and binding energies by a factor of 2–3, with the same values for $N_d$. The variation in the effective masses between compounds is inconsistent with charge-carrier doping in a rigid, parabolic band. This is not entirely unexpected since band hybridization from alkali-metal–Sn bonding has not been taken into consideration. Furthermore, a modification of the conduction-band density of states associated with the distribution of donors is to be expected[24] for donor densities as high as those inferred, $N_d \approx (1.8\text{–}4) \times 10^{20}$ cm$^{-3}$. Some variation in carrier density is also possible for specimens with the same nominal composition in these polycrystalline specimens. Data on single-crystal specimens would be useful in further elucidating this issue. The most reliable mass esti-

TABLE II. Parameters from fits to the impurity-band model described in the text assuming dominant ionized impurity scattering ($\mu \propto T^{3/2}$) and a constant impurity-band mobility $\mu_d$. The units are $N_d$ ($10^{20}$ cm$^{-3}$), $\varepsilon_d$ (meV), $m$ (electron masses), and $\mu$ and $\mu_d$ at 300 K (cm$^2$/V s). The second row of parameters for $Rb_8Zn_4Sn_{42}$ are for the same model, but with a VRH form for $\mu_d$.

| Compound | $N_d$ | $\varepsilon_d$ | $m$ | $\mu$ | $\mu_d$ |
|---|---|---|---|---|---|
| $Cs_8Sn_{44}$ | 4 | 5 | 0.38 | 10 | $4.5\times10^{-2}$ |
| $Cs_8Zn_4Sn_{42}$ | 4 | 10 | 0.45 | 8.3 | $6.0\times10^{-2}$ |
| $Rb_8Zn_4Sn_{42}$ | 4 | 20 | 0.85 | 1.3 | $1.9\times10^{-3}$ |
| | 10 | 30 | 0.85 | 0.7 | $1.3\times10^{-3}$ |
| $Rb_8Ga_8Sn_{38}$ | 1.8 | 3 | 0.14 | 0.6 | $1.0\times10^{-4}$ |

mates come from $Cs_8Sn_{44}$ and $Cs_8Zn_4Sn_{42}$, for which transport properties on several specimens were measured. For comparison, the light and heavy electrons in $\alpha$-Sn are characterized by $m/m_0 = 0.02$ and 0.2, respectively.[25]

The calculated band mobilities at room temperature are quite low, falling in the range $\sim 1$–$5$ cm$^2$/V s. These low values may, in part, be due to scattering from randomly distributed Sn vacancies (in the case of $Cs_8Sn_{44}$) or Ga or Zn atom substitutions on the $6c$ crystallographic site. The consistency of the $N_d$ values for the various specimens suggests that Cs and Rb guest atoms donate roughly the same number of electrons. This number, however, is about one order of magnitude smaller than the nominal value computed assuming one electron per alkali-metal donor atom and using the measured unit cell $N_d \approx 8/(12\times 10^{-8}\ \mathrm{cm}^3) \approx 5\times 10^{21}\ \mathrm{cm}^{-3}$. This discrepancy could be partly due to the compensating effect of acceptors (substitutions or vacancies at the Sn framework sites) which are neglected in the model. Alternatively, the alkali-metal atoms may donate substantially less than one electron due to a more covalent nature of their bonding, suggesting these to be Zintl compounds. The variation in donor energies ($\varepsilon_d$) may reflect different band structures associated with Ga and Zn substitutions in the Sn framework. Including acceptors (and perhaps a contribution from holes), distinguishing the binding energies for Ga and Zn, and incorporating a density of states rather than a discrete level for the impurity band are ingredients for a more sophisticated treatment of these data within the context of the model presented. Finally, we note that a gapless semiconductor model[22] is also capable of reproducing the behavior of the transport coefficients reported here. At present, we view the latter model as less plausible.

## CONCLUSIONS

Temperature-dependent electronic and thermal conductivity measurements on several type-I Sn-clathrate compounds have been reported and discussed. These compounds exhibit low $\kappa$ values that are attributable to the localized disorder associated with the dynamic motion of the alkali-metal atoms. The electronic transport properties were analyzed employing different models and temperature dependences. Guidance from band structure calculations would be useful in further elucidating the electronic transport in these compounds.

## ACKNOWLEDGMENTS

One of the authors (G.S.N.) acknowledges useful discussions with Otto F. Sankey, Jianjun Dong, Charles W. Myles, Glen A. Slack, and H. Julian Goldsmid. This work was supported in part by the U.S. Army Research Laboratory under Contract No. DAAD17-C-99-0006, DARPA under Contract No. N00014-98-3-0011, and Marlow Industries.

[1] G. S. Nolas, J. L. Cohn, G. A. Slack, and S. B. Schujman, Appl. Phys. Lett. **73**, 178 (1998).

[2] J. L. Cohn, G. S. Nolas, V. Fessatidis, T. H. Metcalf, and G. A. Slack, Phys. Rev. Lett. **82**, 779 (1999).

[3] For a recent review see G. S. Nolas, G. A. Slack, and S. B. Schujman, in *Semiconductors and Semimetals*, edited by T. M. Tritt (Academic, New York, 2000), Vol. 69, and references therein.

[4] G. S. Nolas, T. J. R. Weakley, J. L. Cohn, and R. Sharma, Phys. Rev. B **61**, 3845 (2000).

[5] G. S. Nolas, J. L. Cohn, B. C. Chacoumakos, and G. A. Slack, in *Proceedings of the 25th International Thermal Conductivity Conference*, edited by C. Uher and D. T. Morelli (Technomic, Lancaster, PA, 2000), p. 122.

[6] J. S. Tse and M. A. White, J. Phys. Chem. **92**, 5006 (1988).

[7] B. C. Chakoumakos, B. C. Sales, D. G. Mandrus, and G. S. Nolas, J. Alloys Compd. **296**, 801 (1999).

[8] J. Dong and O. F. Sankey, J. Phys.: Condens. Matter **11**, 6129 (1999); J. Dong, O. F. Sankey, G. K. Ramachandran, and P. F. McMillan, J. Appl. Phys. **87**, 7726 (2000).

[9] G. S. Nolas, D. T. Morelli, and T. M. Tritt, Annu. Rev. Mater. Sci. **29**, 89 (1999); C. Uher, in *Semiconductors and Semimetals*, edited by T. M. Tritt (Academic, New York, 2000), Vol. 69.

[10] A. A. Demkov, W. Windl, and O. F. Sankey, Phys. Rev. B **53**, 11 288 (1996) and references therein.

[11] Charles W. Myles, Jianjun Dong, and Otto F. Sankey (private communication).

[12] See, for example, G. D. Mahan, in *Solid State Physics*, edited by H. Ehrenreich and F. Spaepen (Academic, New York, 1998), Vol. 51, p. 81, and references therein.

[13] G. S. Nolas, in *Thermoelectric Materials—The Next Generation Materials for Small-Scale Refrigeration and Power Generation Applications*, edited by T. M. Tritt, G. Mahan, H. B. Lyon, Jr., and M. G. Kanatzidis, Mater. Res. Soc. Symp. Proc. No. 545 (Materials Research Society, Pittsburgh, PA, 1999), p. 435.

[14] G. S. Nolas, T. J. R. Weakley, and J. L. Cohn, Chem. Mater. **11**, 2470 (1999); this reference contains references to all published information on type-I and -II Sn-clathrates up to the time of publication.

[15] G. S. Nolas, B. C. Chakoumakos, B. Mahieu, G. J. Long, and T. J. R. Weakley, Chem. Mater. **12**, 1947 (2000).

[16] *Moffatt's Handbook of Binary Phase Diagrams*, edited by J. H. Westbrook (Genium, New York, 1995), and references therein.

[17] *Numerical Data and Functional Relationships in Science and Technology*, edited by K-.H. Hellwege, Landolt-Börnstein, New Series, Vol. 17a/III (Springer-Verlag, New York, 1982), and references therein.

[18] G. S. Nolas and C. A. Kendziora, Phys. Rev. B **62**, 7157 (2000).

[19] B. B. Iverson, A. E. C. Palmqvist, D. E. Cox, G. S. Nolas, G. D. Stucky, N. P. Blake, and H. Metiu, J. Solid State Chem. **149**, 455 (1999).

[20] N. F. Mott, J. Non-Cryst. Solids **1**, 1 (1968).

[21] H. Fritzsche and M. Cuevas, Phys. Rev. **119**, 1238 (1960).

[22] B. M. Askerov, *Electron Transport Phenomena in Semiconductors* (World Scientific, Singapore, 1994).

[23] See, for example, H. J. Goldsmid, *Electronic Refrigeration* (Pion

Limited, London, 1986), pp. 26–63 or N. Fuschillo, in *Thermoelectric Materials and Devices*, edited by I. B. Cadoff and E. Miller (Reinhold, New York, 1960), pp. 31–46, and references therein.

[24] J. S. Blakemore, *Semiconductor Statistics* (Pergamon, New York, 1962), p. 173.

[25] S. Groves and W. Paul, Phys. Rev. Lett. **11**, 194 (1963); C. F. Lavine and A. W. Ewald, J. Phys. Chem. Solids **32**, 1121 (1971); G. A. Busch and R. Kern, in *Solid State Physics*, edited by F. Seitz and D. Turnbull (Academic, New York, 1960), Vol. 11, p. 1.